# Ramsey Spectroscopy with Displaced Frequency Jumps

M. Shuker,[1,2,*] J. W. Pollock,[1,2] R. Boudot,[3,1] V. I. Yudin,[4,5,6] A. V. Taichenachev,[4,5] J. Kitching,[1,2] and E. A. Donley[1,2]
[1]National Institute of Standards and Technology, Boulder, Colorado 80305, USA
[2]University of Colorado, Boulder, Colorado 80309-0440, USA
[3]FEMTO-ST, CNRS, 26 rue de l'épitaphe 25030 Besancon, France
[4]Novosibirsk State University, ul. Pirogova 2, Novosibirsk, 630090, Russia
[5]Institute of Laser Physics SB RAS, pr. Akademika Lavrent'eva 13/3, Novosibirsk, 630090, Russia
[6]Novosibirsk State Technical University, pr. Karla Marksa 20, Novosibirsk, 630073, Russia

(Received 6 December 2018; revised manuscript received 29 January 2019; published 19 March 2019)

Sophisticated Ramsey-based interrogation protocols using composite laser pulse sequences have been recently proposed to provide next-generation high-precision atomic clocks with a near perfect elimination of frequency shifts induced during the atom-probing field interaction. We propose here a simple alternative approach to the autobalanced Ramsey interrogation protocol and demonstrate its application to a cold-atom microwave clock based on coherent population trapping (*CPT*). The main originality of the method, based on two consecutive Ramsey sequences with different dark periods, is to sample the central Ramsey fringes with frequency jumps finely adjusted by an additional frequency-displacement concomitant parameter, scaling as the inverse of the dark period. The advantage of this displaced frequency-jump Ramsey method is that the local oscillator (LO) frequency is used as a single physical variable to control both servo loops of the sequence, simplifying its implementation and avoiding noise associated with controlling the LO phase. When tested using a *CPT* cold-atom clock, the DFJR scheme reduces the sensitivity of the clock frequency to variations of the light shifts by more than an order of magnitude compared with the standard Ramsey interrogation. This simple method can be applied in a wide variety of Ramsey-spectroscopy based applications including frequency metrology with *CPT*-based and optical atomic clocks, mass spectrometry, and precision spectroscopy.

DOI: 10.1103/PhysRevLett.122.113601

Ramsey's method of separated oscillating fields [1] enables the measurement of atomic and molecular spectral lines with unrivaled precision and accuracy. This widely used spectroscopy and interrogation technique has been successfully applied in a variety of quantum-based measurements and devices including atomic frequency standards [2–7], matter-wave interferometry and atomic inertial sensors [8,9], Bose-Einstein condensates [10], quantum computing [11], memories [12] and information processing [13], cavity quantum electrodynamics [14], optomechanics [15], extreme-ultraviolet spectroscopy [16], mass spectrometry [17], as well as the experimental confirmation of fundamental quantum mechanics concepts [18].

In a typical Ramsey sequence, atoms are probed with two successive pulses separated by a dark period $T$. The first pulse creates a coherence between targeted quantum states whose initial phase is dictated by the external field. During the dark period, a phase shift develops between the atomic coherence and the excitation field determined by their frequency difference and $T$. Through an interference process, the second pulse leads to the modulation of the field absorption spectrum allowing for an effective measurement of the phase difference between the atomic precession and the local oscillator (LO). Scanning the frequency of the excitation field around the exact resonance and measuring the absorption of the second pulse leads to the detection of Ramsey fringes, whose line-width scales as $1/(2T)$.

For clock applications, Ramsey spectroscopy reduces the sensitivity of the clock frequency to variations of the interrogating field [1,19]. However, the Ramsey interrogation exhibits residual frequency shifts induced by the probe field during the interrogation pulses. These interrogation-related shifts originate from a phase shift $\Delta\varphi$ acquired by the atomic coherence during the interrogation pulses. Since the spacing between Ramsey fringes is equal to $1/T$, this phase shift is compensated by an opposite phase shift created by a $1/T$-dependent frequency shift $\Delta f = -\Delta\varphi/(2\pi T)$ between the atomic frequency and the LO frequency during the dark period. These light shifts can be a key limiting factor to the accuracy and long-term frequency stability of atomic clocks based on coherent population trapping (*CPT*) [19–22] and optical clocks that probe ultranarrow quadrupole [23], octupole [24] or two-photon optical transitions [25,26].

*CPT*-based clocks, in which the hyperfine microwave clock-transition frequency is probed using a dual-frequency optical field, are known to suffer from substantial light

 

shifts that depend on the parameters of the optical field. Therefore, a *CPT* clock can serve as a test device for the investigation of interrogation-related shifts and their mitigation. The light shifts in *CPT* clocks originate from resonant interaction of the dual-frequency optical field with the three-level atomic $\Lambda$ scheme [27,28] and from off-resonant coupling of the light field components with neighboring detuned atomic energy levels [29,30]. The resonant shift results from incomplete dark-state formation during the first Ramsey-*CPT* pulse, and can be canceled by increasing the duration or intensity of the first Ramsey pulse [21,27,30,31]. The off-resonant shift, depending mostly on the relative intensity of the two optical frequencies (*CPT* intensity ratio) [32], remains the dominant effect limiting the clock performance.

Over the last decade, sophisticated interrogation protocols based on Ramsey's method have been proposed in order to eliminate probe-induced frequency shifts [33,34]. Among them, the autobalanced Ramsey (ABR) scheme [35] is based on the extraction of two error signals derived from two successive Ramsey sequences with different dark periods. The first feedback loop uses the error signal generated by the short Ramsey sequence to apply a phase-step correction to the LO during the dark period that nulls the probe-field induced frequency shift. The second loop stabilizes the LO frequency using the error signal derived from the long Ramsey sequence. The ABR technique has been applied to different kinds of atomic clocks, demonstrating a significant reduction of the clock frequency sensitivity to light shifts and improving the clock mid- and long-term frequency stability [35–37]. In Ref. [38] a theoretical generalization of the ABR method was presented, demonstrating the possibility to use various concomitant parameters including frequency steps during the Ramsey pulses.

In this Letter, we propose and demonstrate a simple method to reduce interrogation-related frequency shifts in Ramsey spectroscopy that we call Ramsey spectroscopy with displaced frequency jumps (DFJR). Similarly to the techniques presented previously [35,36,38], two servo loops are used to control the clock frequency and a concomitant parameter that suppresses interrogation shifts. However, we propose a way to implement both control parameters with a single physical variable—the LO frequency. Aside from the requirement that the phase of the interrogation field is stable during the Ramsey cycle, no modulation or control of the LO phase is needed. This allows for simpler implementation and the elimination of the systematics associated with controlling and modulating the phase of the oscillator. We also note that the LO frequency remains constant throughout the Ramsey cycle and no rapid control of the LO frequency is required. This method can be applied to any Ramsey spectroscopy measurement, including for *CPT* atomic clocks and optical atomic clocks.

In a Ramsey clock, by sampling the half-height signal on both sides of the central Ramsey fringe with two consecutive Ramsey cycles, a zero-crossing error signal can be derived by subtraction of the two measurements and used to stabilize the frequency of the LO onto the fringe center. Two options are generally used for the generation of the error signal. One option, known as phase jumps, is to abruptly change the phase of the LO between the first and second Ramsey pulse by $\pi/2$ $(-\pi/2)$ during the first (second) Ramsey cycle. Another option, known as frequency jumps, is to jump the frequency of the LO to $1/(4T)$ $[-1/(4T)]$ from the estimated clock frequency during the first (second) Ramsey cycle.

The basic concept of the DFJR method is illustrated in Fig. 1. Figure 1(a) depicts a Ramsey-*CPT* fringe for $T = 16$ ms, probed with standard $\pm 1/(4T)$ frequency-jump interrogation, and assumed to be light shifted by 3 Hz, which results in a similar shift of the stabilized clock frequency. This frequency shift can be eliminated by applying frequency jumps of different magnitude to the

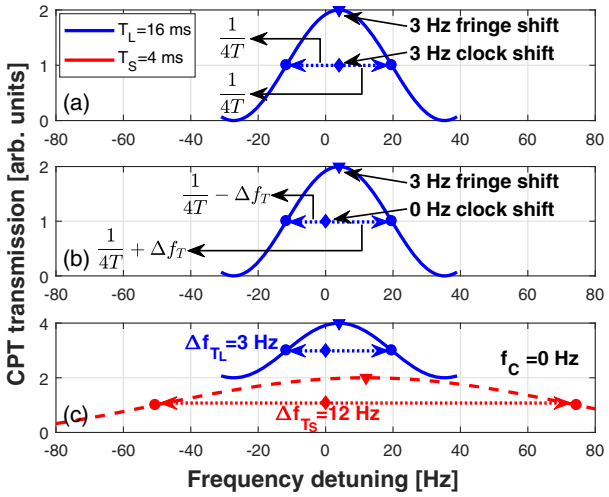


FIG. 1. Illustration of light shifts and their mitigation using the DFJR method. The graphs show the central Ramsey-*CPT* fringes obtained for two different dark periods ($T_L = 16$ ms: blue line and $T_S = 4$ ms: red dashed line). The center of each fringe is marked with a triangle. The steady-state value of the clock frequency is marked with a diamond symbol. Dotted lines show the frequency jumps applied to the sampling frequencies (marked with circles). (a) Light shift with standard Ramsey-*CPT* interrogation ($T = 16$ ms). The clock stabilizes to the shifted Ramsey fringe. (b) By displacing the frequency jumps—jumping a different amount to higher and lower frequencies—the clock frequency shifts can be mitigated. The challenge is then to find the suitable frequency displacement $\Delta f_T$. (c) The DFJR method is used to find $\Delta f_T$ and stabilize the clock frequency on the nonshifted resonance frequency ($f_c = 0$ Hz). Using two different dark periods, $T_S = 4$ ms (lower part of the graph) and $T_L = 16$ ms (upper part of the graph) and adding the frequency displacement $\Delta f_T$ as a $T$-dependent control parameter, the clock frequency is free from light shifts.

right and left sides of the fringe such that the error signal steers the clock to the nonshifted frequency. This approach is demonstrated in Fig. 1(b) where the interrogation asymmetry is denoted by $\Delta f_T$—the frequency displacement which depends on the dark period $T$:

$$\Delta f_T = \frac{\alpha}{T} \tag{1}$$

where $\alpha$ is the concomitant control parameter in the DFJR method. Without prior knowledge of the shifts in the system (which may also vary over time), the difficulty is then to find the correct $\Delta f_T$ value to apply.

For this purpose, the DFJR method consists of a composite Ramsey sequence involving two different dark periods, and uses the measured error signals to find the suitable $\Delta f_T$ value and adapt it over time to compensate drifts in the light shift. We take advantage of the fact that the interrogation-related frequency shifts depend inversely on the dark period. By defining $\Delta f_T$ as a $T$-dependent parameter, the interrogation-related shifts can be distinguished and separated from the clock frequency $f_c$ (which is independent of $T$). We note that frequency shifts that do not scale with $1/T$ (e.g., Zeeman shifts) will not be mitigated by the DFJR method. Figure 1(c) illustrates the principle of the DFJR method. Two Ramsey fringes obtained with a long dark period $T_L = 16$ ms and a short dark period $T_S = 4$ ms are assumed to be light shifted by 3 Hz and 12 Hz, respectively. The frequency jumps are displaced by $\Delta f_{T_L} = (\alpha/T_L)$ and $\Delta f_{T_S} = (\alpha/T_S)$, respectively. Two error signals are then generated (from the short and long cycles) and are used to stabilize the clock frequency $f_c$ and the concomitant control parameter $\alpha$. The only steady-state solution that nulls both error signals occurs when the clock frequency is on resonance, as depicted in Fig. 1(c). This results in a clock frequency free from the influence of interrogation related shifts.

Figure 2 shows the proposed DFJR sequence. It consists of two cycles with a long dark period $T_L$ and two cycles with a short dark period $T_S$. For each pair of cycles, the error signal is generated using frequency jumps from measurements of the half-height signal values on both sides of the central fringe (one value per cycle) and extracting their difference. In the long dark-period cycles, the sampling frequencies are $f_c - [(1/4T_L) - (\alpha/T_L)]$ and $f_c + [(1/4T_L) + (\alpha/T_L)]$, while for the short dark-period cycles the corresponding frequencies are $f_c - [(1/4T_S) - (\alpha/T_S)]$ and $f_c + [(1/4T_S) + (\alpha/T_S)]$. Thus in the DFJR method, one control parameter (the clock frequency, $f_c$) is the same for both dark periods, while the other control parameter, $\alpha$, causes a frequency displacement that scales with the dark period. This allows one to implement two control parameters combined in a single physical variable (the LO frequency). The error signal from the long dark-period cycle pair $\varepsilon_L$ is used to steer the clock frequency, while the error signal from the short dark-period

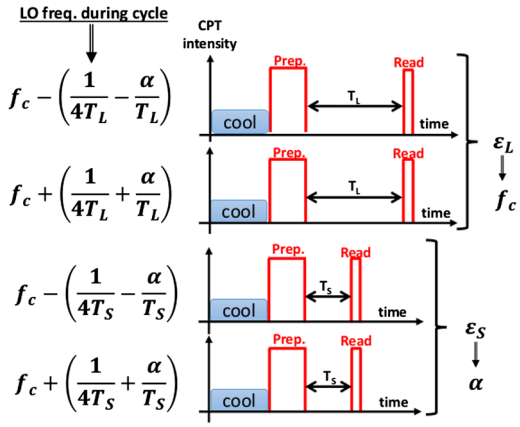


FIG. 2. An illustration of the DFJR sequence, applied to a cold-atom *CPT* clock. The sequence is composed of four consecutive Ramsey cycles—two with a long dark period, $T_L$ and two with a short dark period $T_S$. For each dark period, the two cycles include frequency jumps to the sides of the central fringe. However, the frequency jumps are corrected by a frequency displacement parameter $\Delta f_T$, which scales as the inverse of the dark period [see Eq. (1)]. The frequency for each Ramsey cycle is noted on the left side of the figure. The error signal constructed from the long cycle pair, $\varepsilon_L$, is used to control the clock frequency $f_c$. The error signal derived from the short cycles, $\varepsilon_S$, is used to control the concomitant control parameter $\alpha$.

cycle pair $\varepsilon_S$ is used to steer $\alpha$. In the presence of frequency shifts that depend inversely on the duration of the dark period, the control system will stabilize such that the frequency displacement parameter adapts to compensate these shifts and the clock frequency is free from them. Note that the total DFJR sequence shown in Fig. 2 is symmetrized as reported in Ref. [37] for optimal efficiency of the light-shift rejection.

We implemented the DFJR protocol utilizing a cold-atom clock apparatus previously described in Refs. [21,28]. A six-beam magneto-optical trap is applied for 20 ms followed by a 3 ms molasses, trapping and cooling $\sim 1 \times 10^6$ $^{87}$Rb atoms at a temperature of 10 $\mu$K. At this stage, the atoms are allowed to fall freely and are interrogated in a Ramsey-*CPT* cycle. A 3 ms *CPT* preparation pulse is followed by a dark period $T = 4$–16 ms and a 50 $\mu$s reading *CPT* pulse. We use the lin $\parallel$ lin *CPT* interrogation scheme [39,40] to enhance the *CPT* contrast and retro-reflect the *CPT* beam to minimize Doppler shifts [41]. A quantization magnetic field of $B_z = 4.4$ $\mu$T is applied in the direction of the *CPT* beam propagation. The *CPT* beam is generated from a laser modulated at 6.835 GHz (the Rb ground-state hyperfine splitting frequency) using an electro-optic modulator (EOM). The optical carrier and the $-1$-order sideband are used as the two *CPT* fields. The intensity ratio between the *CPT* fields is controlled using the EOM and measured by a Fabry-Perot interferometer. The intensity and frequency (one-photon detuning, OPD) of the *CPT* beam are controlled

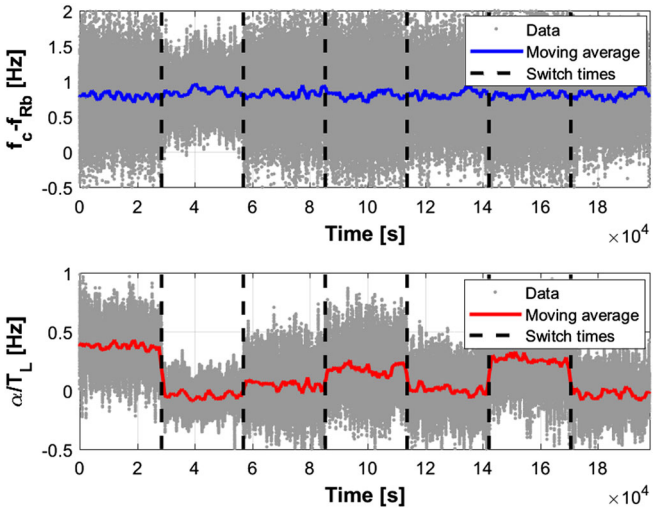


FIG. 3. A time trace of the atomic clock operation based on DFJR. The upper pane shows the clock frequency shift $f_c - f_{Rb}$ and the lower pane shows the frequency displacement for the long cycle $\Delta f_{T_L} = (\alpha/T_L)$. Each pane shows the original data (dots) and a moving average (solid line). During the clock run the *CPT* intensity ratio is abruptly changed (switch times are shown in black dashed lines), changing the off-resonant light shift of the clock transition. It is evident that $\alpha$ adapts to accommodate the changing light shift leaving the clock frequency $f_c$ unaffected (at the value of the second order Zeeman shift).

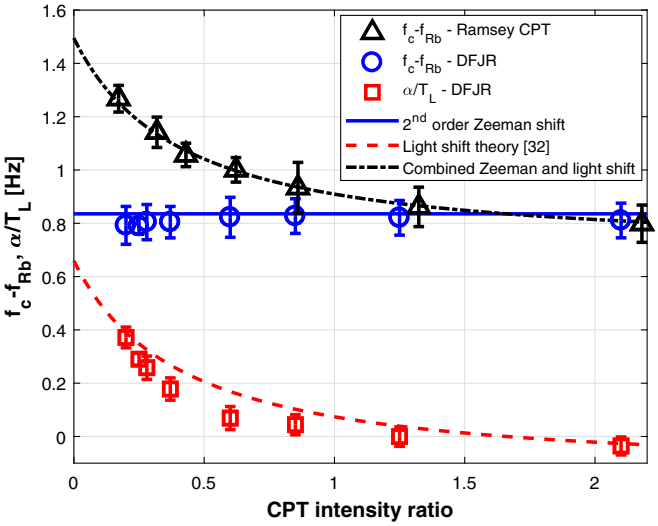


FIG. 4. Frequency shift $f_c - f_{Rb}$ of the clock, in Ramsey-*CPT* (triangles, with $T = 16$ ms) and DFJR (circles, with $T_S = 4$ ms and $T_L = 16$ ms) methods, and frequency displacement for the long cycle $\alpha/T_L$ (squares) versus the *CPT* intensity ratio. In the Ramsey-*CPT* case, the clock frequency is shifted when the *CPT* intensity ratio is changed, due to off-resonant light shift [32]. In the DFJR case, the clock frequency is nearly constant, and $\alpha$ changes to compensate for the light shift. The value of the single control parameter in the Ramsey-*CPT* scheme (the clock frequency) is effectively split into the two control parameters with the DFJR method. The frequency displacement $\Delta f_T$ is associated with the interrogation-related shifts. The clock frequency $f_c$ is free from interrogation related shifts, and is only shifted by the second-order Zeeman shift.

using an acousto-optic modulator. The Ramsey protocols are implemented by controlling the frequency synthesizer driving the EOM. The synthesizer is referenced to a hydrogen maser, and only the frequency of the synthesizer is controlled to implement the protocols. By stabilizing the synthesizer frequency according to the error signals, an atomic clock is obtained and the absolute frequency shifts are measured.

The DFJR method was compared to standard Ramsey-*CPT* spectroscopy by running the cold-atom clock under varying experimental parameters and interrogation shifts. Figure 3 depicts a time trace of DFJR clock operation. The upper pane shows the clock frequency shift, $f_c - f_{Rb}$, where $f_{Rb}$ is the generally accepted unperturbed $^{87}$Rb hyperfine frequency [42], while the lower pane shows the frequency displacement for the long cycle $\Delta f_{T_L} = (\alpha/T_L)$. During clock operation, the off-resonant light shift is altered by abruptly changing the *CPT* intensity ratio. Each time the *CPT* intensity ratio is changed, resulting in a different light shift, the frequency displacement control parameter $\alpha$ stabilizes to a new value, compensating for the light shift, and keeping the clock frequency $f_c$ unaffected. In essence, the two-loop control system keeps one of the control parameters (the clock frequency) protected from this particular kind of systematic.

Figure 4 shows the clock frequency shift $f_c - f_{Rb}$ versus the *CPT* intensity ratio in the standard Ramsey-*CPT* regime ($T = 16$ ms), compared to the DFJR scheme ($T_S = 4$ ms and $T_L = 16$ ms). In the standard Ramsey-*CPT* scheme (triangles) the clock frequency significantly changes with the *CPT* intensity ratio due to the off-resonant light shift [32]. With the DFJR scheme, the frequency displacement parameter $\alpha$ (squares) changes with the *CPT* intensity ratio in order to compensate for the light shift, and the clock frequency (circles) variations are considerably reduced. The absolute clock frequency shift is then about 0.835 Hz, in good agreement with the expected second-order Zeeman shift in the lin $\parallel$ lin configuration (which is $T$ independent and hence not canceled).

We also tested the ability of the DFJR method to mitigate light shifts that depend on the *CPT* laser OPD. For this purpose, we applied sinusoidal oscillations to the OPD with an amplitude of $\pm 1$ MHz and a period of about 2 h ($\sim 1.4 \times 10^{-4}$ Hz frequency) during clock operation. Figure 5 shows the fast Fourier transform (FFT) spectrum of the clock frequency for the Ramsey-*CPT* and DFJR methods. In the Ramsey-*CPT* case, a strong peak is observed at the OPD oscillation frequency whereas the amplitude of this peak is reduced by an order of magnitude in the DFJR method. It is interesting to note that the FFT noise spectrum of the DFJR clock frequency shows an increased noise level. We attribute this degradation to the

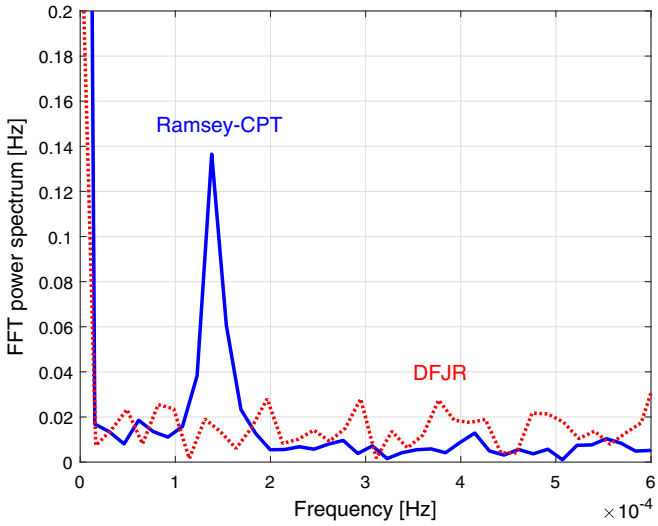


FIG. 5. FFT power spectra of the clock frequency in Ramsey-*CPT* (with $T = 16$ ms) and DFJR ($T_S = 4$ ms, $T_L = 16$ ms) methods. Sinusoidal oscillations with an amplitude of $\pm 1$ MHz and about 2 h period are applied to the OPD of the *CPT* laser. An order-of-magnitude reduction of the oscillations amplitude is observed with the DFJR method.

longer clock sequence in the DFJR method, resulting in a slightly degraded short-term stability. This effect was previously observed in ABR-*CPT* clocks [36].

In conclusion, we demonstrated a simple method to reduce interrogation-related shifts in Ramsey spectroscopy and tested it using a cold-atom *CPT* clock. The so-called displaced frequency jump Ramsey spectroscopy scheme relies on the fact that interrogation-related frequency shifts depend inversely on the dark period and is based on Ramsey interrogations with different dark periods. Using frequency jumps, the first servo loop nulls the probing-field induced frequency shift by adding a slight frequency displacement that scales with $1/T$ while the second servo loop stabilizes the LO frequency. This approach presents the benefit of controlling only a single physical variable (the frequency of the LO), simplifying implementation and eliminating the noise associated with controlling the LO phase. A significant reduction by more than an order of magnitude of the clock frequency dependence to variations of the *CPT* intensity ratio and of the laser OPD has been observed with the DFJR scheme, in comparison with the standard Ramsey-*CPT* scheme.

The authors acknowledge V. Maurice, S. Brewer, J. Elgin, and C. Oates for review of the manuscript and helpful discussions. Russian team was supported by the Russian Science Foundation (No. 16-12-10147). V. I. Y. was also supported by the Ministry of Education and Science of the Russian Federation (No. 3.1326.2017/4.6), and Russian Foundation for Basic Research (No. 17-02-00570). A. V. T. was also supported by Russian Foundation for Basic Research (No. 18-02-00822). R. B. was supported by the NIST Guest Researcher fellowship and Délégation Générale de l'Armement (DGA). This work is a contribution of NIST, an agency of the U.S. government, and is not subject to copyright.

*moshe.shuker@nist.gov

[1] N. F. Ramsey, Phys. Rev. **78**, 695 (1950).
[2] J. E. Thomas, P. R. Hemmer, S. Ezekiel, C. C. Leiby, R. H. Picard, and C. R. Willis, Phys. Rev. Lett. **48**, 867 (1982).
[3] G. Santarelli, P. Laurent, P. Lemonde, A. Clairon, A. G. Mann, S. Chang, A. N. Luiten, and C. Salomon, Phys. Rev. Lett. **82**, 4619 (1999).
[4] T. Zanon, S. Guérandel, E. de Clercq, D. Holleville, N. Dimarcq, and A. Clairon, Phys. Rev. Lett. **94**, 193002 (2005).
[5] T. L. Nicholson, S. L. Campbell, R. B. Hutson, G. E. Marti, B. J. Bloom, R. L. McNally, W. Zhang, M. D. Barrett, M. S. Safronova, G. F. Strouse, W. L. Tew, and J. Ye, Nat. Commun. **6**, 6896 (2015).
[6] N. Nemitz, T. Ohkubo, M. Takamoto, I. Ushijima, M. Das, N. Ohmae, and H. Katori, Nat. Photonics **10**, 258 (2016).
[7] M. Schioppo, R. C. Brown, W. F. McGrew, N. Hinkley, R. J. Fasano, K. Beloy, T. H. Yoon, G. Milani, D. Nicolodi, J. A. Sherman, N. B. Phillips, C. W. Oates, and A. D. Ludlow, Nat. Photonics **11**, 48 (2017).
[8] F. Riehle, T. Kisters, A. Witte, J. Helmcke, and C. J. Bordé, Phys. Rev. Lett. **67**, 177 (1991).
[9] V. Ménoret, P. Vermeulen, N. L. Moigne, S. Bonvalot, P. Bouyer, A. Landragin, and B. Desruelle, Sci. Rep. **8**, 12300 (2018).
[10] E. A. Donley, N. R. Claussen, S. T. Thompson, and C. E. Wieman, Nature (London) **417**, 529 (2002).
[11] J. Lim, H. Lee, S. Lee, C. Y. Park, and J. Ahn, Sci. Rep. **4**, 5867 (2014).
[12] X. Maitre, E. Hagley, G. Nogues, C. Wunderlich, P. Goy, M. Brune, J. M. Raimond, and S. Haroche, Phys. Rev. Lett. **79**, 769 (1997).
[13] P. Schindler, D. Nigg, T. Monz, J. T. Barreiro, E. Martinez, S. X. Wang, S. Quint, M. F. Brandl, V. Nebendahl, C. F. Roos, M. Chwalla, M. Hennrich, and R. Blatt, New J. Phys. **15**, 123012 (2013).
[14] S. Deleglise, I. Dotsenko, C. Sayrin, J. Bernu, M. Brune, J. M. Raimond, and S. Haroche, Nature (London) **455**, 510 (2008).
[15] K. Qu, C. Dong, H. Wang, and G. S. Agarwal, Phys. Rev. A **90**, 053809 (2014).
[16] A. Pirri, E. Sali, C. Corsi, M. Bellini, S. Cavalieri, and R. Eramo, Phys. Rev. A **78**, 043410 (2008).
[17] G. Bollen, H.-J. Kluge, T. Otto, G. Savard, and H. Stolzenberg, Nucl. Instrum. Methods Phys. Res., Sect. B **70**, 490 (1992).
[18] S. Gleyzes, S. Kuhr, C. Guerlin, J. Bernu, S. Deléglise, U. B. Hoff, M. Brune, J.-M. Raimond, and S. Haroche, Nature (London) **446**, 297 (2007).
[19] M. Abdel Hafiz, G. Coget, P. Yun, S. Guérandel, E. de Clercq, and R. Boudot, J. Appl. Phys. **121**, 104903 (2017).

[20] P. Yun, F. Tricot, C. E. Calosso, S. Micalizio, B. Francois, R. Boudot, S. Guérandel, and E. de Clercq, Phys. Rev. Applied **7**, 014018 (2017).
[21] X. Liu, E. Ivanov, V. I. Yudin, J. Kitching, and E. A. Donley, Phys. Rev. Applied **8**, 054001 (2017).
[22] X. Liu, V. I. Yudin, A. Taichenachev, J. Kitching, and E. A. Donley, Appl. Phys. Lett. **111**, 224102 (2017).
[23] Y. Huang, J. Cao, P. Liu, K. Liang, B. Ou, H. Guan, X. Huang, T. Li, and K. Gao, Phys. Rev. A **85**, 030503 (2012).
[24] K. Hosaka, S. A. Webster, A. Stannard, B. R. Walton, H. S. Margolis, and P. Gill, Phys. Rev. A **79**, 033403 (2009).
[25] M. Fischer, N. Kolachevsky, M. Zimmerman, R. Holzwarth, T. Udem, T. W. Hansch, M. Abgrall, J. Grunert, I. Maksimovic, S. Bize, H. Marion, F. P. Dos Santos, P. Lemonde, G. Santarelli, P. Laurent, A. Clairon, C. Salomon, M. Haas, U. D. Juentschura, and C. H. Keitel, Phys. Rev. Lett. **92**, 230802 (2004).
[26] T. Badr, M. D. Plimmer, P. Juncar, M. E. Himbert, Y. Louyer, and D. J. E. Knight, Phys. Rev. A **74**, 062509 (2006).
[27] P. R. Hemmer, M. S. Shahriar, V. D. Natoli, and S. Ezekiel, J. Opt. Soc. Am. B **6**, 1519 (1989).
[28] E. Blanshan, S. M. Rochester, E. A. Donley, and J. Kitching, Phys. Rev. A **91**, 041401(R) (2015).
[29] Y. Yano, W. J. Gao, S. Goka, and M. Kajita, Phys. Rev. A **90**, 013826 (2014).
[30] G. S. Pati, Z. Warren, N. Yu, and M. S. Shahriar, J. Opt. Soc. Am. B **32**, 388 (2015).
[31] S. M. Shahriar, P. R. Hemmer, D. P. Katz, A. Lee, and M. G. Prentiss, Phys. Rev. A **55**, 2272 (1997).
[32] J. W. Pollock, V. I. Yudin, M. Shuker, M. Y. Basalaev, A. V. Taichenachev, X. Liu, J. Kitching, and E. A. Donley, Phys. Rev. A **98**, 053424 (2018).
[33] V. I. Yudin, A. V. Taichenachev, C. W. Oates, Z. W. Barber, N. D. Lemke, A. D. Ludlow, U. Sterr, C. Lisdat, and F. Riehle, Phys. Rev. A **82**, 011804 (2010).
[34] T. Zanon-Willette, R. Lefèvre, R. Metzdorff, N. Sillitoe, S. Almonacil, M. Minisalle, E. de Clercq, A. V. Taichenachev, V. I. Yudin, and E. Arimondo, Rep. Prog. Phys. **81**, 094401 (2018).
[35] C. Sanner, N. Huntemann, R. Lange, C. Tamm, and E. Peik, Phys. Rev. Lett. **120**, 053602 (2018).
[36] M. Abdel Hafiz, G. Coget, M. Petersen, C. Rocher, S. Guérandel, T. Zanon-Willette, E. de Clercq, and R. Boudot, Phys. Rev. Applied **9**, 064002 (2018).
[37] M. Abdel Hafiz, G. Coget, M. Petersen, C. Calosso, S. Guérandel, E. de Clercq, and R. Boudot, Appl. Phys. Lett. **112**, 244102 (2018).
[38] V. I. Yudin, A. V. Taichenachev, M. Y. Basalaev, T. Zanon-Willette, J. W. Pollock, M. Shuker, E. A. Donley, and J. Kitching, Phys. Rev. Applied **9**, 054034 (2018).
[39] A. V. Taichenachev, V. I. Yudin, V. L. Velichansky, and S. A. Zibrov, JETP Lett. **82**, 398 (2005).
[40] S. A. Zibrov, I. Novikova, D. F. Phillips, R. L. Walsworth, A. S. Zibrov, V. L. Velichansky, A. V. Taichenachev, and V. I. Yudin, Phys. Rev. A **81**, 013833 (2010).
[41] F. X. Esnault, E. Blanshan, E. N. Ivanov, R. E. Scholten, J. Kitching, and E. A. Donley, Phys. Rev. A **88**, 042120 (2013).
[42] F. Riehle, P. Gill, F. Arias, and L. Robertsson, Metrologia **55**, 188 (2018).